TS measurements of *ex-situ* yellowfin tuna *(Thunnus albacares)* and frequency-response discrimination for tropical tuna species

Bea Sobradillo [1], Guillermo Boyra [2], Jon Uranga [2] and Gala Moreno [3]

[1]*AZTI, Marine Research, Basque Research and Technology Alliance (BRTA), Txatxarramendi Ugartea Z/G, Sukarrieta, Spain*

[2]*Azti, AZTI, Marine Research, Basque Research and Technology Alliance (BRTA), Muelle de la Herrera, Zona Portuaria s/n – 20110 Pasaia, Gipuzkoa, Spain*

[3]*International Seafood Sustainability Foundation (ISSF), 3706 Butler Street Suite #316, 15201-1820 Pittsburgh, PA (USA)*

Abstract

Tuna fisheries support one of the world's most valuable markets, with over 50% of the catch coming from drifting fish aggregating devices (DFADs). To locate and quantify tuna on DFADs, fishermen mostly use acoustic technologies, which significantly reduce the nominal fishing effort, especially in tropical purse seine fisheries. However, to date, discrimination between species using purely acoustic methods has not been refined due to a lack of information on the acoustic response of each species at different frequencies. Three tuna species can be found simultaneously at DFADs: skipjack or SKJ (*Katsuwanus pelamis*), bigeye or BET (*Thunnus obesus*), and yellowfin or YFT (*Thunnus albacares*), of which only the acoustic frequency responses of SKJ and BET have been published. In this study, we present the frequency response obtained from ex situ measurements of YFT recorded at 38, 70, 120 and 200 kHz. Records based on two data sets were used to describe the relationship between acoustic signal or target strength (TS; dB re $1m^2$) and fish length across frequencies. The results described a flat response across frequencies, with b20 (standard deviation) values of -72.4 (9), -73.2 (8), -72.3 (8), and -72.3 (9) dB at 38, 70, 120, and 200 kHz, respectively. These results, combined with previously published increasing (SKJ) and decreasing (BET) responses, were used to develop a discrimination algorithm for these 3 species. The algorithm was tested using acoustic data and catches from commercial campaigns aboard a tuna vessel.

Introduction

More than half of the purse seine landings targeting tropical tunas come from fishing with Fish Aggregating Devices (DFADs). These have sophisticated acoustic sensors on board (vertical and side-looking echosounders, as well as long-range multibeam sonar) in addition to satellite buoys equipped with low-cost acoustic echosounders, to allow fishermen to decide on which FAD to visit. The use of acoustic devices before setting the nets improves the selectivity of the catch (Lopez *et al.*, 2014; Moreno *et al.*, 2016). However, few studies have been published on the acoustic characteristics of the species present at DFADs (Bertrand, 1999; Lu *et al.*, 2011; Boyra *et al.*, 2018, 2019), and most of the recorded data are currently underutilized, hampering their potential to provide information on the location, composition and abundance of species from a distance. There are mainly three tropical tuna species that can be aggregated simultaneously in DFADs (Fonteneau *et al.*, 2013): skipjack or SKJ (*Katsuwanus pelamis*), bigeye or BET (*Thunnus obesus*), and yellowfin or YFT (*Thunnus albacares*). Since 2014, AZTI, in collaboration with ISSF, has been conducting a series of studies to improve the discrimination between species and the determination of average size of tuna using both echosounder data and sonar from the tuna vessels themselves. The first step in developing acoustic methods for species discrimination is to determine the sound scattering properties of each species separately, which are mainly defined by the backscattering cross-section (σ_{bs}; m^2) and its logarithmic form, the target strength (TS; dB re 1 m^2] (MacLennan *et al.*, 2002). So far, during the four surveys conducted (three in the Atlantic and one in the Pacific), it has been possible to determine the acoustic characteristics of two of the three main species fished in the DFADs: skipjack (Boyra et al., 2018) and bigeye tuna (Boyra et al., 2019), and to take the first steps towards the acoustic discrimination of tropical tunas (Moreno *et al.*, 2019). The main objective of the present work is to determine the acoustic properties, mainly the TS(*f*) and TS(*L*) relationships, of small-sized yellowfin tunas in captivity and combine them with the previously published results of SKJ and BET to develop an acoustic discrimination algorithm for tropical tunas (Moreno *et al.*, 2019).

Materials and methods

The experiments were conducted at the IATTC Achotines Laboratory, located in Achotines Bay, Panama **(Figure 1)**. The first measurements were made in July 2016 (days 27, 28 and 29), and the final measurements were between May 24 and June 22 of year

2022. The experiments were conducted in an *offshore* cage with a diameter of 25 meters and a depth of just under 20 meters. The experiments consisted of capturing yellowfin tuna, transporting them alive to the cage and then recording measurements with scientific acoustic equipment to study the acoustic characteristics of this species.

Biological sampling. Once the acoustic measurements were completed, the cage was dismantled and all specimens were removed for biological sampling (length, width, height and weight of each fish) and X-rays to study the swimbladder morphology **(Figure 2, Table 1)**.

Acoustic sampling. A Simrad EK60 scientific echosounder with three split-beam transducers at 38, 120 and 200 kHz was used in 2016, and an EK80 with four split-beam transducers (38, 70, 120 and 200 kHz) was used for the 2022 measurements. All transducers had a 7-degree opening beam and were vertically oriented downwards with an emitted pulse duration of 0.512 ms in CW mode. The maximum nearfield effect was determined as the sum of the emitted and backscattered fields, from the transducer and the fish body, respectively. With this in mind, and being rather conservative, the minimum depth at which data were considered reliable in this study was set at 10 m.

The transducers were mounted on a steel plate, with a flotation system and a weight to keep it stable below the surface line. The electronics were installed on a vessel with a battery system for power supply and awnings to protect the computers from sunlight and rain. Calibration was performed prior to data collection, using a 38.1 mm tungsten sphere at a depth of 24.5 m with the settings specified in **Table 2** and following the standard target method (Demer *et al.*, 2015).

Data analysis. Acoustic recordings for TS estimation and TS-length relationship were made on live tuna in both the 2016 and 2022 sets **(Table 1,** Error! Reference source not found.**)**. The study of the acoustic characteristics of live yellowfin tuna was conducted using target strength analysis (Simmonds and MacLennan, 2005), which consists of obtaining the echo of isolated yellowfin tuna targets in the 10-25 m depth range. The echosounder data were processed using commercial (Echoview; Hobart, Tasmania) and an open-source software (R, R Core Team, 2014). A single target detection algorithm (MacLennan and Menz, 1996; Soule *et al.*, 1996; Demer *et al.*, 1999) was used to discard unwanted echoes. The threshold for data analysis was set to -50 dB and other parameters were left as their default values (see **Table 3**). In addition, a target tracking analysis (Blackman, 1986) (see **Table 3**) was used to assign individual target detections to individual tracks and to obtain the fish orientation by comparing the displacements along the horizontal and vertical axes of the first and last echoes of each track.

The relationship between TS and fork length was modeled as a linear regression of the type:

$$TS = a \log_{10}(L) + b, \quad \textbf{(Eq. 1)}$$

where the slope (a) was assumed to be 20 due to the small number of length samples available, insufficient to generate an experimental slope. The b_{20} (Simmonds and MacLennan, 2005) of yellowfin tuna was estimated for each frequency using the averaged length measurements. However, the central TS value per frequency was obtained as the mode of the TS histogram, after smoothing to a Gaussian density curve. This was done first to remove the effect of possible noise in the distribution, but also to remove the effect of the minimum threshold on the final central value. The mode of the distribution was then retained and used to obtain the TS(L) relationship.

Frequency response-based discrimination algorithm. Two elements were used to develop a discrimination algorithm for the three major tropical tuna species: (1) the individual frequency response patterns of the three species and (2) an optimization process to determine the interspecific classification limits of the algorithm. The frequency response patterns of each individual species were obtained from the literature in the case of SKJ and BET (Boyra et al., 2018, 2019; Moreno et al., 2019) and from the present study for YFT, and were defined in terms of differences in mean volume backscattering strength (ΔMVBS) between frequency pairs **(Eq. 2)**. These individual responses were used to define generic classification rules dependent on undefined thresholds (to be defined in the optimization process):

$$Species = \begin{cases} SKJ,\ if & \begin{cases} MVBS_{38} - MVBS_{200} < A \\ MVBS_{38} - MVBS_{120} < B \end{cases} \\ BET,\ if & \begin{cases} MVBS_{38} - MVBS_{200} > C \\ MVBS_{38} - MVBS_{120} > D \end{cases} \\ YFT,\ if & \begin{cases} A < MVBS_{38} - MVBS_{200} < C \\ MVBS_{38} - MVBS_{120} < D \end{cases} \end{cases} \quad \textbf{(Eq. 2)}$$

To obtain the thresholds that optimized the algorithm performance, each condition was tested against multiple values to retain the thresholds that minimized the root mean square error (RMSE) between the predicted and observed species proportions. Once the optimal thresholds were defined, the RMSE metric was used to estimate the mask classification performance, both overall and by species.

Results and discussion

Biological sampling. A total of 6 specimens were used in the experiments (**Table 1**). Mean fork lengths of sets 1 and 2 were 52.7 cm and 51.4 cm, respectively. The swimbladder was elongated, from 2 to 3 times longer than it was wide and occupied approximately 21% (± 2.5) of the body length. It was tilted 25 ± 5 degrees from the horizontal axis of the body **(Figure 2)**.

TS distributions. The TS distributions observed from the measurements of live tuna in the cage had a spread of more than 20 dB in all frequencies, with the widest spread observed at 200 kHz **(Figure 5)**. The median values showed a relatively flat frequency response at 38, 120 and 200 kHz in set 1, and at 38, 70 and 120 kHz in set 2. The median value at 200 kHz was 3 dB higher in set 2 than in set 1 **(Figure 5)**. When combining both sets, the smoothed Gaussian distributions produced central mode TS values at -38 dB at 38 kHz, -40 dB at 70 kHz, -36 dB at 120 kHz and 38 dB at 200 kHz **(Figure 6)**. These values were used to fit the TS(*L*) model for each frequency resulting in b_{20} values of -72.4 (9), -73.2 (8), -72.3 (8) and -72.3 (9) dB, resulting in flat responses across the frequency band **(Figure 7)**. There were differences among the TS distributions across the two sets of this study despite the similarity in mean length between both **(Table 1)**. Possible reasons for this difference may be attributed to differences in tilt angle distribution between both sets. Alternatively, it could be due to the different individual size composition between the two experiments. In 2016 there were 4 tuna in the cage, including one large and one small tuna. Whereas in 2022 there were only two tuna of almost the same size in the cage. Perhaps the representativeness of the larger tuna was higher in the first experiment because it was easier to meet the conditions of the single-target algorithm, which may have biased the result towards higher TS values. Or it may simply be the natural variability of TS. It is commonly assumed that TS depends on fish size according to a specific relationship **(Eq. 1)**, with two parameters that are defined as a function of the growth rate of the resonance organs compared to the growth rate of the fish. Yellowfin tuna of under nearly 2 kg do not present a gas-filled swimbladder, which may lead to unprecise estimations of TS-length relationships, however, in this study, all the specimens were above 2 kg in weight **(Table 1)** and presented a well-developed swimbladder as could be observed in the X-ray images. Several authors have recommended empirically fitting both parameters of the TS-length relationship for each species and length range, because the variation of TS with size may follow different patterns (Midttun, 1984; Bertrand, 2000; Lu *et al.*, 2011; Sobradillo *et al.*, 2019). However, whether both parameters can be determined empirically depends on the availability of fish length measurements associated with echo detections. When data are scarce, as length was in the present study, it is widely assumed that the acoustic cross-section is proportional to the horizontal cross-section of the swimbladder, which is also proportional to the square of the fish length (Simmonds and MacLennan, 2005). This

relationship implies that the slope in **Eq. 1** is set to 20, and only the intercept (b_{20}) is empirically determined. This simplification also allows the acoustic signal of the three tuna species of interest to be more easily compared.

TS versus tilt angle. A total of 312 tracks were used to extract the fish orientation and analyze the variation of TS versus the apparent tilt angle of the fish. A Loess smoothing was fit to the angle distribution, obtaining maximum TS (-37.5 ± 0.5 dB) for angles between -15 and -30 degrees **(Figure 8)**, and a minimum TS (-43 ± 0.5 dB) for angles between 25 and 40 degrees. Approximately 80% of the tracks were detected within a range of 0 ± 20 degrees. Only a small number of tracks, 6% of the total, deviated significantly from this pattern, being tilted more than 60 degrees either upwards or downwards. The contribution of the fish orientation to the variability of the TS values is a well-known issue (Dahl and Mathisen, 1983) that is mainly related to fish behaviour (McQuinn and Winger, 2003). Both analyses were consistent with previous studies (Bertrand, 1999; Lu *et al.*, 2011; Puig-Pons *et al.*, 2022) in that the highest backscatter was observed when tuna were descending with the swimbladder largest cross-section oriented perpendicular to the transducer beam **(Figure 8)**.

Frequency response of three tropical tuna. These results were combined with the previously published frequency response of BET and SKJ (Moreno *et al.*, 2019) **(Figure 9)**, which showed that BET presented the highest b_{20} values of the three species at 38 and 120 kHz (-65.3 ± 8 and -65.6 ± 7 dB), with a decrease of almost 7 dB at 200 kHz. Conversely, the frequency response described by SKJ was low at 38 kHz (-76 dB) and increased by almost 6 dB at high frequencies. YFT described a flat frequency response, with variations of less than 1 dB across frequencies. In general, the BET response decreased with frequency, the SKJ response increased and the YFT response remained relatively flat across frequencies **(Figure 9)**. The increasing or flat response is typical for swimbladdered fish (Fernandes *et al.*, 2006) as well as of other large physoclists (Pedersen *et al.*, 2004). On the other hand, SKJ does not have a swimbladder, which explains the increasing response pattern with frequency, as is the case in other non-swimbladdered species (Mosteiro *et al.*, 2004; Fernandes *et al.*, 2006; Korneliussen, 2010; Forland *et al.*, 2014).

Discrimination algorithm. Four different thresholds were obtained for each combination of frequencies used to resolve each of the three species according to **Eq. 2**. According to them, a cell of the echogram was attributed to SKJ when the echointegrated energy was, at least, -2.4 dB (threshold A) higher at 200 kHz than at 38 kHz, and -1.2 dB (threshold B) higher at 120 kHz than at 38 kHz. Cells with values that were at least 0.72 dB higher at 38 kHz than at 200 kHz and 0.36 dB higher at 120 kHz than at 200 kHz were assigned to BET. Finally, cells were classified to YFT if the difference between 38 kHz and 200 kHz was within -2.4 dB and 0.72 dB, or below 0.36 dB between 120 kHz and 200 kHz.

The applied mask resulted in a deviation of less than 10% from the observed proportions of the species. The highest accuracy in classification was obtained for skipjack tuna (SKJ), with the least variation from the actual proportions. BET tended to be overestimated, while YFT tended to be slightly underestimated **(Figure 10)**. Regarding the overall performance of the mask, the RMSE was 21.1%. The RMSE for BET and SKJ was close to 27%, while for YFT it was 20.1% **(Figure 11)**. These results are consistent with the first steps presented in *Moreno et al.* (2019), where echo integrated *Sv* values were used to describe the frequency response. As stated in the same study, some uncertainty will always remain as part of the stochasticity inherent in the target strength (Simmonds and MacLennan, 2005), but the monospecific acoustic records of yellowfin tuna collected in this study contributed significantly to reducing the uncertainty by increasing the acoustic dataset, as recommended therein. In addition, the availability of split-beam echosounders for TS estimation, as well as the reduced (or nonexistent) risk of detecting unresolved multiple targets (Soule *et al.*, 1996; Ona, E. and Barange, M., 1999), has greatly increased the potential of the knowledge gained, not only for species discrimination, but also for estimating the abundance of species present in the DFADs.

Relevance of this work for selective fishing: This work represents the culmination of the line of research aimed at acoustic identification of the three primary tropical tuna species commonly found associated with DFADs. The data collected from this study, along with previous research conducted within the same line of investigation (Boyra *et al.*, 2018, 2019; Moreno *et al.*, 2019), can be readily utilized to identify the presence of BET, SKJ, and YFT around DFADs, as well as calculate their relative abundances. This knowledge can greatly enhance the sustainability of tropical tuna, when implemented in the acoustic technology used by purse seine vessels.

Acknowledgements

We would like to express our gratitude to the staff at the Achotines laboratory for the invaluable logistic help and for their daily effort in searching for tuna. We also thank Xiker Salaberria, Iker Urtizberea and Udane Martinez for their help, which was essential to carry out the entire data collection process. This project received funding from the Economic Development, Sustainability and Environment Department, as well as from the vice ministry of Agriculture, Fisheries and Food Policy, Fisheries and Aquaculture Directorate of the Basque Government. Funding was also received under award NA19NMF4720214 from the 2019 Bycatch Reduction Engineering Program NOAA from National Marine Fisheries Service (NMFS) and National Oceanic and Atmospheric Administration (NOAA); and had the additional support of the International Seafood Sustainability Foundation (ISSF).

Bibliography

Aglen, A. 1994. Sources of error in acoustic estimation of fish abundance. Marine Fish Behaviour in Capture and Abundance Estimation. Fishing.: 107–133. News Books.

Baidai, Y., Dagorn, L., Amande, M. J., Gaertner, D., and Capello, M. 2020a. Machine learning for characterizing tropical tuna aggregations under Drifting Fish Aggregating Devices (DFADs) from commercial echosounder buoys data. Fisheries Research, 229: 105613. Elsevier.

Baidai, Y., Dagorn, L., Amandè, M. J., Gaertner, D., and Capello, M. 2020b. Tuna aggregation dynamics at Drifting Fish Aggregating Devices: a view through the eyes of commercial echosounder buoys. ICES Journal of Marine Science, 77: 2960–2970.

Baidai, Y. 2021. Derivation of a direct abundance index for tropical tunas based on their associative behavior with floating objects Yannick Diby Armel Baidai To cite this version : HAL Id : tel-03166452 DE L ' UNIVERSITÉ DE M ONTPELLIER Derivation of a direct abundance i.

Barclay, K., and Cartwright, I. 2007. Governance of tuna industries: The key to economic viability and sustainability in the Western and Central Pacific Ocean. Marine Policy, 31: 348–358.

Bard, F.-X., Bach, P., and Josse, E. 1998. Habitat, ecophysiologie des thons : quoi de neuf depuis 15 ans ?

Bertrand, A., Josse, E., and Masse, J. 1999. In situa coustic target-strength measurement of bigeye (Thunnus obesus) and yellowfin tuna (Thunnus albacares) by coupling split-beam echosounder observations and sonic tracking. ICES Journal of Marine Science, 56: 51–60.

Bertrand, A. 2000. Tuna target-strength related to fish length and swimbladder volume. ICES Journal of Marine Science, 57: 1143–1146.

Blackman, S. S. 1986. Multiple-target tracking with radar applications. Dedham, MA, Artech House, Inc., 1986, 463 p.

Boyra, G., Moreno, G., Sobradillo, B., Pérez-Arjona, I., Sancristobal, I., and Demer, D. A. 2018. Target strength of skipjack tuna (Katsuwanus pelamis) associated with fish aggregating devices (FADs). ICES Journal of Marine Science, 75: 1790–1802.

Boyra, G., Moreno, G., Orue, B., Sobradillo, B., and Sancristobal, I. 2019. In situ target strength of bigeye tuna (Thunnus obesus) associated with fish aggregating devices. ICES Journal of Marine Science: fsz131.

Boyra, G., Martínez, U., Uranga, J., Moreno, G., and Peña, H. 2023. Correction of beam overlap-induced athwart distortion in multibeam sonars. ICES Journal of Marine Science, 80: 197–209.

Castro, J. J., Santiago, J. A., and Santana-Ortega, A. T. 2002. A general theory on fish aggregation to floating objects: An alternative to the meeting point hypothesis. Reviews in Fish Biology and Fisheries, 11: 255–277.

CMM 2021-01. 2022. Conservation and Management Measure for Tropical Tunas.

Dahl, P., and Mathisen, O. 1983. Measurement of fish target strength and associated directivity at high frequencies. The Journal of the Acoustical Society of America, 73: 1205–1211. Acoustical Society of America.

Dawson, J. J., and Karp, W. A. 1990. In situ measures of target-strength variability of individual fish. ICES (International Council for the Exploration of the Sea) Cooperative Research Report, 189: 264–273.

Dawson, J. J., Wiggins, D., Degan, D., Geiger, H., Hart, D., and Adams, B. 2000. Point-source violations: split-beam tracking of fish at close range. Aquat. Living Resour.

Demer, D. A., Soule, M. A., and Hewitt, R. P. 1999. A multiple-frequency method for potentially improving the accuracy and precision of in situ target strength measurements. The Journal of the Acoustical Society of America, 105: 2359–2376.

Demer, D. A., Berger, L., Bernasconi, M., and Eckhard, B. 2015. Calibration of acoustic instruments. ICES Cooperative Research Report, 326: 136.

Escalle, L., Vidal, T., Heuvel, B. V., Clarke, R., Hare, S., Hamer, P., and Pilling, G. 2021. 1 Oceanic Fisheries Programme, The Pacific Community (SPC), Noumea, New Caledonia 2 Cape Fisheries; 3 South Pacific Tuna Corporation (SPTC).

Fernandes, P., Korneliussen, R., Lebourges-Dhaussy, A., Masse, J., Iglesias, M., Diner, N., Ona, E., *et al.* 2006. The SIMFAMI project: species identification methods from acoustic multifrequency information. Final Report to the EC, 2054.

Fonteneau, A., Pallarés, P., and Pianet, R. 2000. A worldwide review of purse seine fisheries on FADs.

Foote, K. G. 1985. Rather-high-frequency sound scattering by swimbladdered fish. The Journal of the Acoustical Society of America, 78: 688–700.

Foote, K. G. 2014. Discriminating between the nearfield and the farfield of acoustic transducers. The Journal of the Acoustical Society of America, 136: 1511–1517.

Forland, T. N., Hobæk, H., and Korneliussen, R. J. 2014. Scattering properties of Atlantic mackerel over a wide frequency range. ICES Journal of Marine Science, 71: 1904–1912.

Freon, P., and Dagorn, L. 2000. Review of fish associative behaviour: toward a generalisation of the meeting point hypothesis. Reviews in Fish Biology and Fisheries, 10: 183–207.

Furusawa, M. 1988. Prolate spheroidal models for predicting general trends of fish target strength. Journal of the Acoustic Society of Japan, 9.

Furusawa, M., Hamada, M., and Aoyama, C. 1999. Near Range Errors in Sound Scattering Measurements of Fish. Fisheries science, 65: 109–116.

Gaertner, D., Clermidy, S., Ariz, J., Bez, N., Moreno, G., Murua, H., Soto, M., *et al.* 2018. Results achieved within the framework of the EU research project: Catch, Effort, and eCOsystem impacts of FAD-fishing (CECOFAD).

Galland, G., Rogers, A., and Nickson, A. 2016. Netting billions: a global valuation of tuna. The Pew Charitable Trusts. https://www.pewtrusts.org/-/media/assets/2016/05/netting_billions.pdf.

Gastauer, S., Scoulding, B., and Parsons, M. 2017. Estimates of variability of goldband snapper target strength and biomass in three fishing regions within the Northern Demersal Scalefish Fishery (Western Australia). Fisheries Research, 193: 250–262.

Gerlotto, F., and Fréon, P. 1992. Some elements on vertical avoidance of fish schools to a vessel during acoustic surveys. Fisheries Research, 14: 251–259.

Godø, O. R., and Michalsen, K. 2000. Migratory behaviour of north-east Arctic cod, studied by use of data storage tags. Fisheries Research, 48: 127–140.

Hazen, E. L., and Horne, J. K. 2003. A method for evaluating the effects of biological factors on fish target strength. ICES Journal of Marine Science, 60: 555–562.

IATTC. 2021. Resolution C-21-04 Conservation measures for tropical tunas in the Eastern Pacific Ocean during 2022-2024. https://www.iattc.org/GetAttachment/e3dc0a7e-e73c-4b8e-889e-a4cd2cdd7b8b/C-21-04-Active_Tuna-conservation-in-the-EPO-2022-2024.pdf (Accessed 7 July 2023).

ICCAT. 2019. Reportof the 2019 ICCAT yelowfin tuna stock assessment meeting.. 8–16. YELLOWFIN TUNA SA MEETING- GRAND BASSAM.

ICCAT. 2021. Recommendation by ICCAT replacing recommendation 19-02 replacing recommendation 16-01 on a multi-annual conservation and management programme for tropical tunas. 1–21. https://www.iccat.int/Documents/Recs/compendiopdf-e/2021-01-e.pdf (Accessed 7 July 2023).

ICCAT. 2021. Report of the 2021 bigeye stock assessment meeting. 19–29. BET STOCK ASSESSMENT MEETING- -ONLINE.

IOTC. 2019. Resolution 19/02 Procedures on a Fish Aggregating Devices (FADs) management plan. 1–11. https://faolex.fao.org/docs/pdf/mul199458.pdf (Accessed 7 July 2023).

IOTC 19-01. 2019. Resolution 19/01 on an interim plan for rebuilding the Indian Ocean Yellowfin tuna stock in the IOTC area of competence. Indian Ocean Tuna Commission.

IOTC 23-04. 2023. Resolution 23/04 on an interim plan for rebuilding the Indian Ocean Yellowfin tuna stock in the IOTC area of competence. Indian Ocean Tuna Commission.

ISSF. 2023. ISSF Workshop on different approaches to limit the number of FADs in the oceans. ISSF Technical report, 2023–03. ISSF, Pittsbourgh, PA, USA.

Itano, D. 2003. Documentation and classification of fishing gear and technology on board tuna purse seine vessels. *In* 16th Sixteenth Meeting of the Standing Committee on Tuna and Billfish (SCTB16), held in Mooloolaba, Queensland, Australia, pp. 9–16.

Knudsen, F. R., Fosseidengen, J. E., Oppedal, F., Karlsen, Ø., and Ona, E. 2004. Hydroacoustic monitoring of fish in sea cages: target strength (TS) measurements on Atlantic salmon (Salmo salar). Fisheries Research, 69: 205–209.

Komeyama, K., Kadota, M., Torisawa, S., Suzuki, K., Tsuda, Y., and Takagi, T. 2011. Measuring the swimming behaviour of a reared Pacific bluefin tuna in a submerged aquaculture net cage. Aquatic Living Resources, 24: 99–105.

Komeyama, K., Kadota, M., Torisawa, S., and Takagi, T. 2013. Three-dimensional trajectories of cultivated Pacific bluefin tuna Thunnus orientalis in an aquaculture net cage. Aquaculture Environment Interactions, 4: 81–90.

Korneliussen, R. J. 2010. The acoustic identification of Atlantic mackerel. ICES Journal of Marine Science: Journal du Conseil, 67: 1749–1758.

Lopez, J., Moreno, G., Sancristobal, I., and Murua, J. 2014. Evolution and current state of the technology of echo-sounder buoys used by Spanish tropical tuna purse seiners in the Atlantic, Indian and Pacific Oceans. Fisheries Research, 155: 127–137.

Lu, H.-J., Kang, M., Huang, H.-H., Lai, C.-C., and Wu, L.-J. 2011. Ex situ and in situ measurements of juvenile yellowfin tuna Thunnus albacares target strength. Fisheries Science, 77: 903–913.

MacLennan, D., Fernandes, P. G., and Dalen, J. 2002. A consistent approach to definitions and symbols in fisheries acoustics. ICES Journal of Marine Science, 59: 365–369.

MacLennan, D. N., and Menz, A. 1996. Interpretation of in situ target-strength data. ICES Journal of Marine Science: Journal du Conseil, 53: 233–236.

Mannocci, L., Baidai, Y., Forget, F., Tolotti, M. T., Dagorn, L., and Capello, M. 2021. Machine learning to detect bycatch risk: Novel application to echosounder buoys data in tuna purse seine fisheries. Biological Conservation, 255: 109004.

McQuinn, I. H., and Winger, P. D. 2003. Tilt angle and target strength: target tracking of Atlantic cod (Gadus morhua) during trawling. ICES Journal of Marine Science, 60: 575–583.

Midttun, L. 1984. Fish and other organisms as acoustic targets. *In* pp. 25–33.

Misund, O. A., Øvredal, J. T., and Hafsteinsson, M. T. 1996. Reactions of herring schools to the sound field of a survey vessel. Aquatic Living Resources, 9: 5–11.

Moreno, G., Dagorn, L., Capello, M., Lopez, J., Filmalter, J., Forget, F., Sancristobal, I., *et al.* 2016. Fish aggregating devices (FADs) as scientific platforms. Fisheries Research, 178: 122–129.

Moreno, G., Boyra, G., Sancristobal, I., Itano, D., and Restrepo, V. 2019. Towards acoustic discrimination of tropical tuna associated with Fish Aggregating Devices. PLOS ONE, 14: e0216353.

Mosteiro, A., Fernandes, P. G., Armstrong, F., and Greenstreet, S. P. R. 2004. A dual frequency algorithm for the identification of sandeel school echotraces. ICES Document CM, 12: 1–13.

Mulligan, T. 2000. Shallow water fisheries sonar: a personal view. Aquatic Living Resources, 13: 269–273.

Nucci, M., Costa, C., Scardi, M., and Cataudella, S. 2010. Preliminary observations on bluefin tuna (Thunnus thynnus, Linnaeus 1758) behaviour in captivity. Journal of Applied Ichthyology, 26: 95–98. Wiley Online Library.

Ona, E. 1990. Physiological factors causing natural variations in acoustic target strength of fish. Journal of the Marine Biological Association of the United Kingdom, 70: 107–127. Cambridge University Press.

Ona, E. and Barange, M. 1999. Single target recognition. CRR, Methodology for Target Strength Measurement. http://www.ices.dk/sites/pub/Publication%20Reports/Cooperative%20Research%20Report%20(CRR)/crr235/CRR235.pdf (Accessed 28 February 2017).

Pedersen, G., Korneliussen, R. J., and Ona, E. 2004. The relative frequency response, as derived from individually separated targets on cod, saithe and Norway pout. ICES. http://brage.bibsys.no/xmlui/handle/11250/100629 (Accessed 25 February 2016).

Pérez-Arjona, I., Godinho, L. M. C., and Espinosa, V. 2018. Numerical Simulation of Target Strength Measurements from Near to Far Field of Fish Using the Method of Fundamental Solutions. Acta Acustica united with Acustica, 104: 25–38.

Pons, M., Kaplan, D., Moreno, G., Escalle, L., Abascal, F., Hall, M., Restrepo, V., *et al.* 2023. Benefits, concerns and solutions of fishing for tunas with drifting fish aggregating devices. Fish and Fisheries.

Precioso, D., Navarro-García, M., Gavira-O'Neill, K., Torres-Barrán, A., Gordo, D., Gallego, V., and Gómez-Ullate, D. 2022. TUN-AI: Tuna biomass estimation with Machine Learning models trained on oceanography and echosounder FAD data. Fisheries Research, 250: 106263.

Puig-Pons, V., Muñoz-Benavent, P., Pérez-Arjona, I., Ladino, A., Llorens-Escrich, S., Andreu-García, G., Valiente-González, J. M., *et al.* 2022. Estimation of Bluefin Tuna (Thunnus thynnus) mean length in sea cages by acoustical means. Applied Acoustics, 197: 108960.

Rodríguez-Sánchez, V., Encina-Encina, L., Rodríguez-Ruiz, A., and Sánchez-Carmona, R. 2016. Do close range measurements affect the target strength (TS) of fish in horizontal beaming hydroacoustics? Fisheries Research, 173: 4–10.

Rose, G. A., and Porter, D. R. 1996. Target-strength studies on Atlantic cod (Gadus morhua) in Newfoundland waters. ICES Journal of Marine Science, 53: 259–265. Oxford University Press.

Santiago, J., Uranga, J., Quincoces, I., Orue, B., Grande, M., Murua, H., Merino, G., *et al.* 2019. A Novel Index of Abundance of Skipjack in the Indian Ocean Derived From Echosounder Buoys. IOTC-2019-WPTT21-45.

Schaefer, K. M. 1999. Comparative study of some morphological features of yellowfin (Thunnus albacares) and bigeye (Thunnus obesus) tunas. Inter-American Tropical Tuna Commission.

Simmonds, E. J., and MacLennan, D. N. 2005. Fisheries acoustics: theory and practice. Fish and aquatic resources series. Blackwell Science, Oxford ; Ames, Iowa. 437 pp.

Sobradillo, B., Boyra, G., Martinez, U., Carrera, P., Peña, M., and Irigoien, X. 2019. Target Strength and swimbladder morphology of Mueller's pearlside (Maurolicus muelleri). Scientific Reports, 9: 1–14.

Soule, M., Hampton, I., and Barange, M. 1996. Potential improvements to current methods of recognizing single targets with a split-beam echo-sounder. ICES Journal of Marine Science: Journal du Conseil, 53: 237–243.

Uranga, J., Lopez, J., Santiago, J., Boyra, G., Maunder, M. N., Murua, H., Grande, M., *et al.* 2022. TROPICAL TUNA BIOMASS INDICATORS FROM ECHOSOUNDER BUOYS IN THE EASTERN PACIFIC OCEAN.

Zhang, J., Chen, Z., Chen, G., Zhang, P., Qiu, Y., and Yao, Z. 2015. Hydroacoustic studies on the commercially important squid Sthenoteuthis oualaniensis in the South China Sea. Fisheries research, 169: 45–51. Elsevier.

Zhang, J., Zhang, K., Chen, Z., Dong, J., and Qiu, Y. 2021. Hydroacoustic studies on Katsuwonus pelamis and juvenile Thunnus albacares associated with light fish-aggregating devices in the South China Sea. Fisheries Research, 233: 105765.

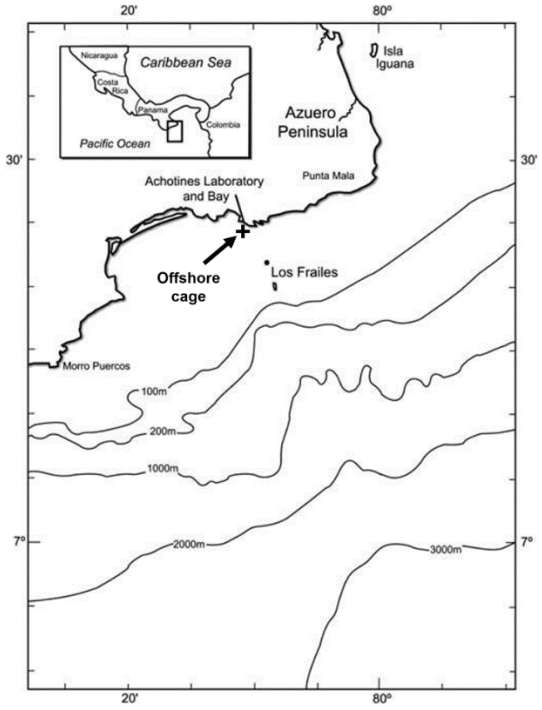

Figure 1. Location of the offshore cage outside Achotines Bay.

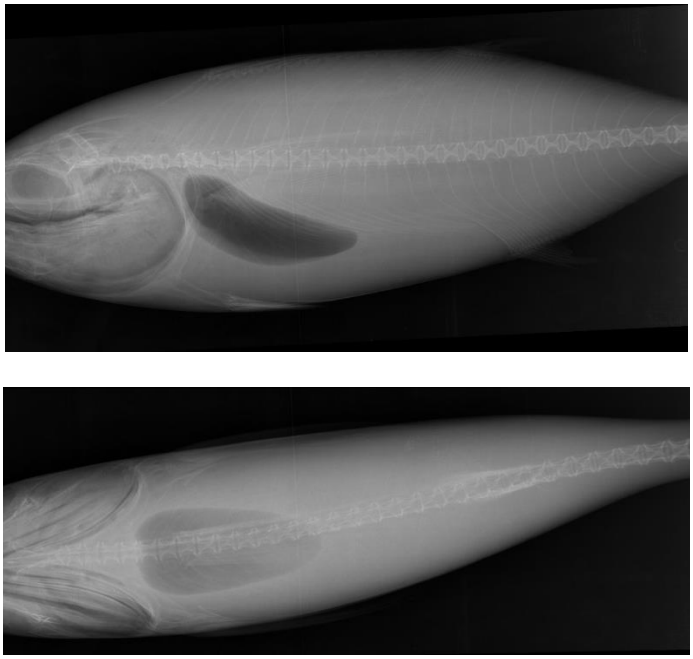

Figure 2. Example radiograph of one of the tunas in the cage, showing the morphology of the swim bladder in lateral (a) and ventral (b) views.

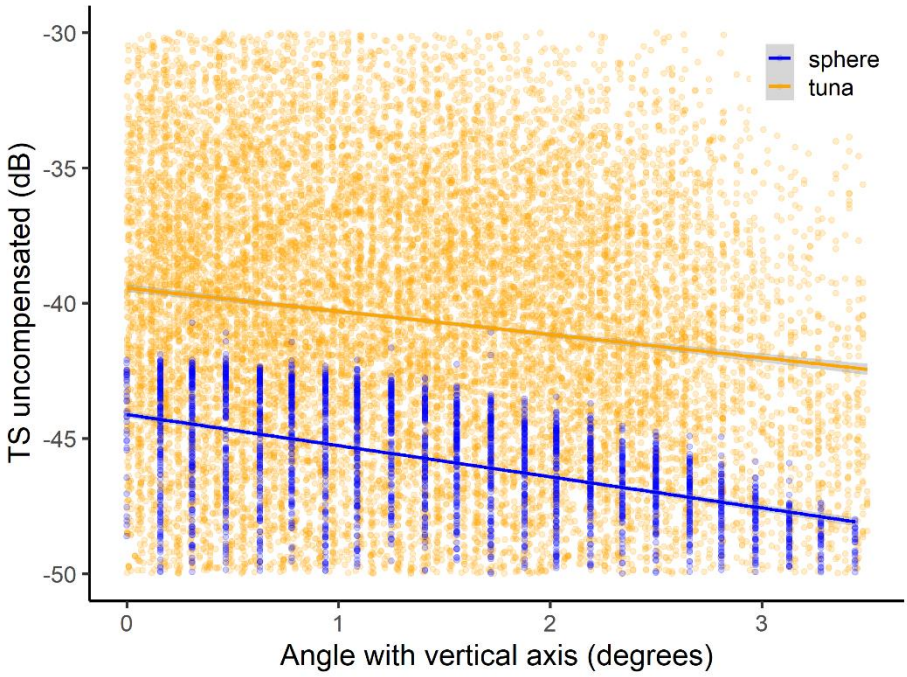

Figure 3. Comparison of uncompensated TS values from the calibration sphere and tuna targets located at different positions in the beam. The resulting slopes are the same for both targets, which

means that the split-beam transducer is able to locate the target at the operating depth regardless of the size of the measured target.

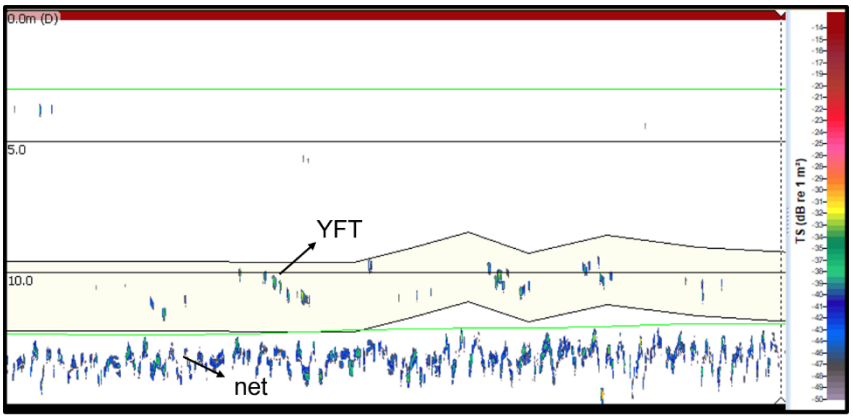

Figure 4. 38 kHz echogram showing the yellowfin tuna echoes close to the bottom of the cage.

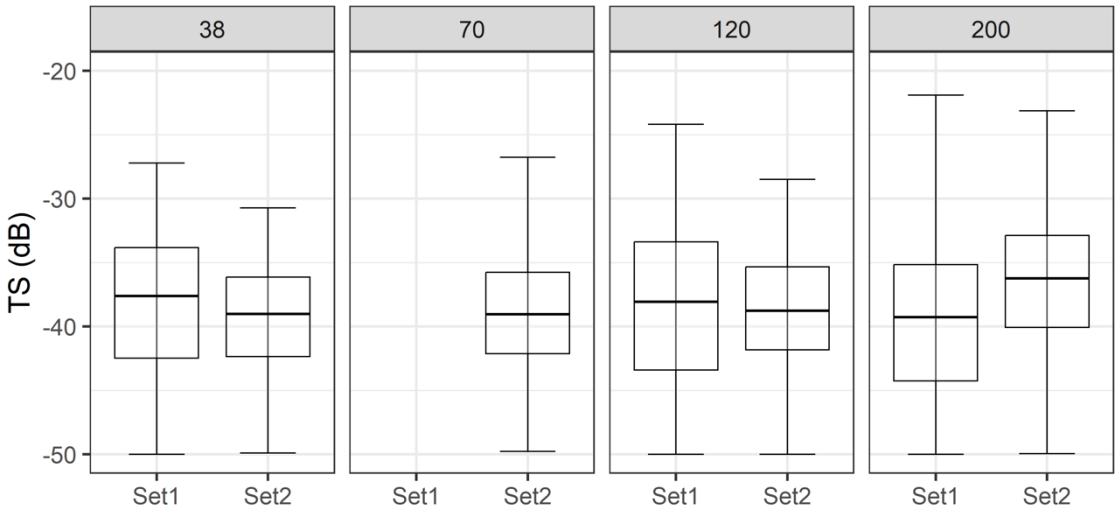

Figure 5. TS boxplots of the single targets from the two sets of measurements at the four operational frequencies (kHz), showing the first, second and third quartiles of the distributions.

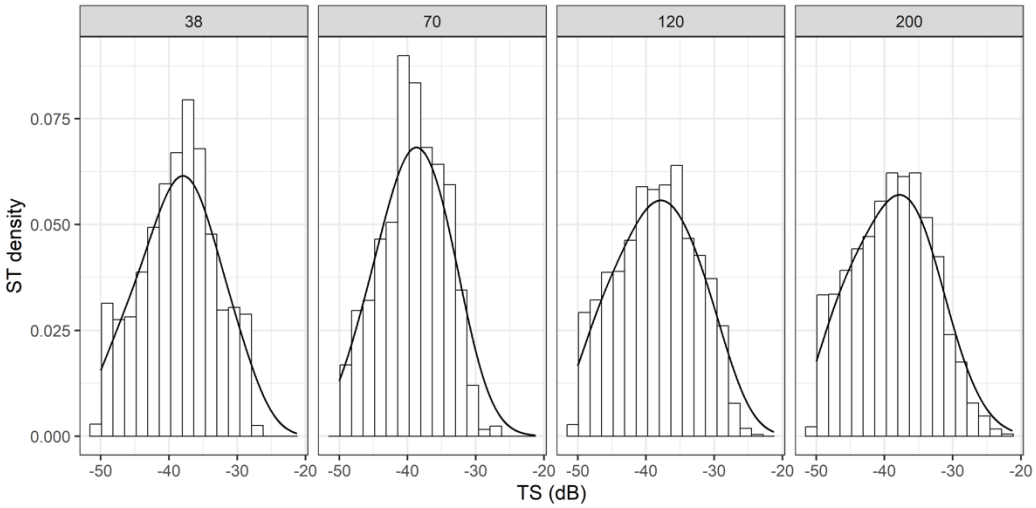

Figure 6. TS distribution with density curves obtained from single targets, filtered at -50 dB at the four operational frequencies (kHz).

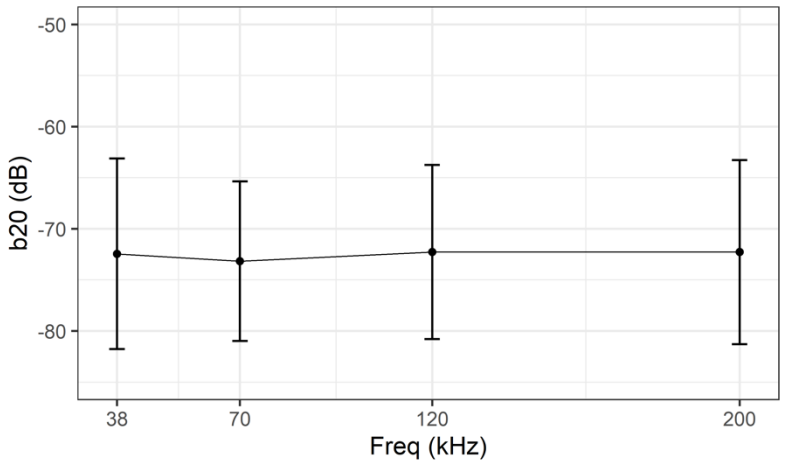

Figure 7. Frequency response of the mode of b_{20} values obtained from yellowfin tuna single target detections at the four frequencies of study.

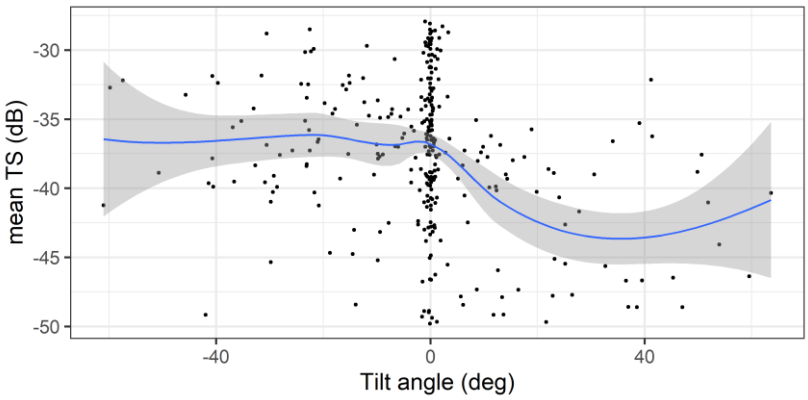

Figure 8. Mean TS variation against tilt angle at the four operational frequencies obtained from set 1, at 38 kHz. Tracks were filtered to -50 dB and a loess smoothing was applied.

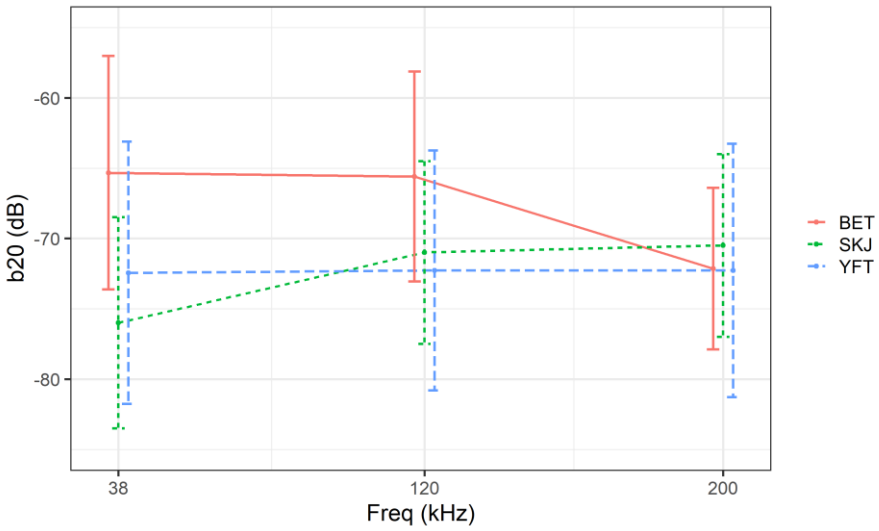

Figure 9. Frequency response of the b_{20} values from BET, YFT and SKJ. Error bars illustrate the standard deviation.

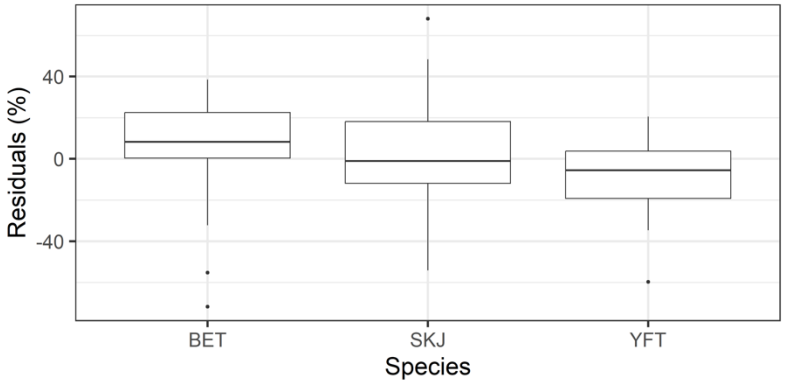

Figure 10. Residuals of the discrimination algorithm per species.

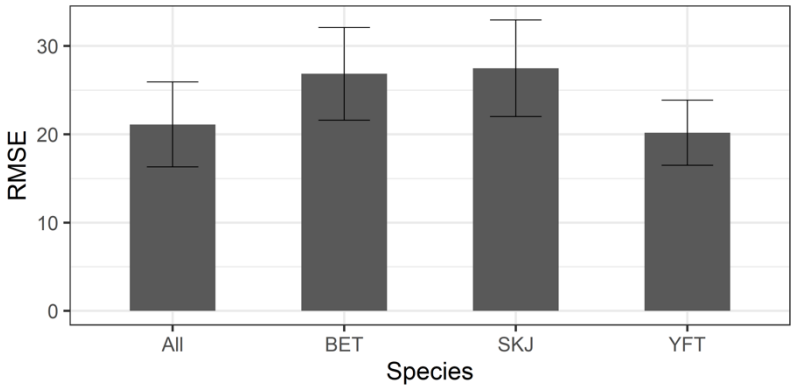

Figure 11. Error (RMSE) of the mask performance calculated by species and overall error. The errorbars indicate +/- one standard error of the mean.

Table 1.Biological measurements from fish body (TL: total length, FL: fork length, width, height and weight), and swimbladder. Z is the depth at which the diameter of the acoustic beam cross-section equals the fish or swimbladder length. Specimen marked with (*) is dead and used for controlled range experiment.

		Fish						Swimbladder			
Year	**Set**	**TL**	**FL**	**Z**	**Width**	**Height**	**Weight**	**Length**	**Z**	**Width**	**Area**
		cm	cm	m	cm	cm	kg	cm	m	cm	cm^2
2016	1	57	51.9	4.7	9.5	13	2.9	11.4	0.9	3.1	28.0
2016	1	70.8	64.4	5.8	11	15	3.9	12.2	1.0	4.1	38.8
2016	1	45.2	41.1	3.7	7.5	10.5	1.52	9.3	0.8	2.7	19.8
2016	1	59	53.7	4.8	10	13.5	3.16	12.5	1.0	3.8	37.6
2022	2	58	54.4	4.7	9.3	13.4	5.8	13.0	1.1	3.2	32.7
2022	2	56.2	51.4	4.6	8.5	13.2	5.25	10.7	0.9	3.4	28.6

Table 2.Calibrated echosounder settings used for measurements.

Year	Units	2016			2022			
Frequency	kHz	38	120	200	38	70	120	200
Pulse duration	µs	512	512	512	512	512	512	512
Power	W	2000	250	150	2000	750	250	150
Gain	dB	26.62	27	26.2	26.76	27	25.8	25.5
Sa correction	dB	-1.19	-0.41	-0.39	-0.59	-0.26	-0.11	-0.22
Sphere TS	dB	-42.04	-39.83	-39.45	-42.04	-40.56	-39.83	39.45

Table 3.Parameters used in the single target detection (SED) and tracking algorithms.

SED algorithm			Tracking algorithm		
Pulse length determination level	dB	6	Min. number of single targets in a track		3
Min/max normalized pulse length		0.7/1.5	Max number of pings in a track	pings	3
Maximum beam compensation	dB	3	Maximum gap between single targets	pings	5
Maximum standard deviation of axis angles	degrees	0.6	Exclusion distance (major axis/minor axis/range)	m	4/4/0.1